J Membrane Biol (2014) 247:627–638
DOI 10.1007/s00232-014-9680-x

Niflumic Acid Affects Store-Operated Ca^{2+}-Permeable (SOC) and Ca^{2+}-Dependent K^+ and Cl^- Ion Channels and Induces Apoptosis in K562 Cells

Yuliya V. Kucherenko · Florian Lang

Received: 28 October 2013 / Accepted: 10 May 2014 / Published online: 25 May 2014

Abstract Non-steroidal anti-inflammatory drugs (NSAIDs) are known to induce apoptosis in a variety of cancer cells. However, the precise mechanisms by which NSAIDs facilitate apoptosis in tumor cells are not clear. In the present study, we show that niflumic acid (NA), a member of the fenamates group of NSAIDs and Cl^- and Ca^{2+}-activated Cl^- (CAC) channels blocker, induced apoptosis (by ~8 %, 24 h treatment) and potentiated (by 8–10 %) apoptotic effect of endoplasmic reticulum Ca^{2+} mobilizer thapsigargin (Tg) in human erythroleukemic K562 cell line. The whole-cell patch clamp and Fluo-3 flow cytometric experiments confirmed an inhibitory effect of NA (100 and 300 μM) on store-operated (SOC) channels. We also found that NA-blocked CAC channels were activated by acute application of Tg (2 μM) in K562 cells. NA blockage of CAC channels was accompanied by activation of Ca^{2+}-activated K^+ (SK4) channels. The observed effects of NA were not connected with COX-2 inhibition since 100-nM NA (IC_{50} for COX-2 inhibition) did not induce either apoptosis or affect the channels activity. We conclude that inhibition of SOC channels plays a major role in NA-induced apoptosis. Increased apoptotic levels in Tg-treated K562 cells in the presence of NA may be due to the blockage of CAC and stimulation of SK4 channels in addition to SOC channels inhibition.

Y. V. Kucherenko (✉)
Institute for Problems of Cryobiology and Cryomedicine, Kharkov 71015, Ukraine
e-mail: yulia_kucherenko@yahoo.com

F. Lang
Department of Physiology Institute I, Eberhard-Karls Universität Tübingen, 72076 Tübingen, Germany

Keywords K562 cells · Niflumic acid · Apoptosis · CAC · SK4 · SOC channels

Introduction

Non-steroidal anti-inflammatory drugs (NSAIDs) are known to induce apoptosis in a variety of cancer cells, including colon, gastric, glioma, pancreatic, and lung cancer cells (Cao and Prescott 2002). Most of NSAIDs demonstrate strong COX-2 and COX-1 inhibitory effects. COX-2 is up-regulated in a number of cancers (colon, breast, lung, pancreas, and carcinoma). The excessive production of prostaglandins, mainly PGE_2, enhances tumor cell growth. Anti-tumor effect of NSAIDs treatment was suggested to result in COX-2 inhibition and thus accumulation of intracellular arachidonic acid that induces apoptosis by involvement of caspase-3 and a transition of mitochondrial permeability. However, recent studies showed that apoptotic effect of NSAIDs is COX-2 independent since the drugs induced apoptosis at much higher concentrations than their IC_{50} for COX-2 inhibition (Totzke et al. 2003). In addition, NSAIDs caused apoptosis in COX-2 deficient cells and a number of NSAIDs that demonstrated no COX-2 inhibition, nevertheless, were effective in apoptosis induction.

COX-2 specific inhibitors (nimesulide, NS-398, celecoxib) were shown to induce apoptosis of haematopoietic cancer cells (Cerella et al. 2011; Subhashini et al. 2005; Zhang et al. 2006). The effect was COX-2 independent since no suppression of low basal PGE_2 production upon the treatment was observed (Cerella et al. 2011). Celecoxib (10–100 μM) was shown to induce apoptosis in K562 cells via release of cytochrome C into the cytoplasm and cleavage of poly (ATP-ribose) polymerase-1 (PARP-1) followed by DNA fragmentation. Bcl-2 level was declined and NF-kB activation was

inhibited (Subhashini et al. 2005). Another study on celecoxib-induced apoptosis in K562 cells demonstrated caspase-3 activation with increasing doses of celecoxib. However, inhibition of caspase-3 activity did not abolish the celecoxib-induced apoptosis that suggests a caspase-independent pathway of the cells apoptosis (Zhang et al. 2006).

Niflumic acid (NA), a selective COX-2 inhibitor, belongs to the fenamates group of NSAIDs (Liantonio et al. 2006). It is widely used in medical practice for dysmenorrhea, rheumatoid, and osteoarthritis treatment.

The recent study demonstrated that combined NA and PARPγ-ligand ciglitazone treatment synergistically induced apoptotic cell death in human lung cancer cells and it was realized through COX-2 and PARPγ-independent mechanisms. Endoplasmic reticulum (ER) stress and caspase-8 activation were critical in combined NA-ciglitazone treatment-induced apoptosis (Kim et al. 2011).

Laboratory studies showed that NA modulates activity of Ca^{2+}-activated Cl^- channels (CAC), e.g., CLC-1 channel in skeletal muscle cells (Astill et al. 1996; Liantonio et al. 2007), CLC-K channel in kidney cells (Liantonio et al. 2006; Wangemann et al. 1986), TMEM16A channel in HEK293 cells (Chen et al. 2011), bestrophin-2 (Best2) channel in mouse olfactory sensory neurons (Pifferi et al. 2006). In addition, NA affects the activity of large- (BK_{Ca}) and intermediate-conductance (IK_{Ca}) Ca^{2+}-activated K^+ channels in vascular smooth muscle cells (Li et al. 2008a, b), and endothelial cells (Ahn et al. 2004). NA was also shown to induce changes in $[Ca^{2+}]_i$ in neurons, smooth muscle cells, gastric mucosal cells by affecting intracellular Ca^{2+} stores (Poronnik et al. 1992; Tomisato et al. 2004), and activating ryanodine-sensitive Ca^{2+} release channels (Li et al. 2008b).

The data concerning apoptotic effect of NA on haematopoietic cancer cells are missing.

In the present study, we show that NA, at concentrations higher than that for COX-2 inhibition, induced apoptosis and potentiated apoptotic effect of known ER mobilizing agent Tg in human erythroleukemic K562 cell line. We address the question of ion channels involvement in apoptotic effect of NA in K562 cells.

Materials and Methods

Cell Culturing

K562 cells (kind gift of Dr. Topp, department of Hematology, Oncology, Immunology and Reumatology, University Medical center, University of Tuebingen, Germany) were grown in 1 % L-glutamine containing RPMI 1640 medium (Gibco, Karlsruhe, Germany) supplemented with 10 % FCS and 1 % penicillin/streptomycin.

Where indicated, Tg (2 μM), niflumic acid (NA; 100 nM, 100, and 300 μM) were added to the cell culture medium. Ethanol, a solvent for NA, was added at the same concentration to controls.

Phosphatidylserine Exposure

Phosphatidylserine exposure (PS exposure) was determined in the cells stained with Annexin V-Fluos (ImmunoTools, Friesoythe, Germany) as it was described by the manufacturer. Briefly, the cells (up to 10^6) were washed in 500-μl 5 mM Ca^{2+} containing binding buffer for 5 min at $250\times g$. The supernatant was discarded, the cell pellet was re-suspended in 70-μl 5 mM Ca^{2+} containing binding buffer, 5 μl of Annexin V-FITC was added and the cells were incubated for 15 min at room temperature in dark. Then, the cell suspension was diluted (1:4) with the same binding buffer and measured by flow cytometric analysis (FACS-Calibur from Becton–Dickinson; Heidelberg, Germany) in fluorescence channel FL-1 with an excitation wavelength of 488 nm and an emission wavelength of 530 nm.

Intracellular Ca^{2+}

For $[Ca^{2+}]_i$ measurements K562 cells were washed with 5 mM Ca^{2+} containing NaCl Ringer bath solution, and then loaded with 1-μM Fluo-3/AM (Biotium, Hayward, USA). Then, the cells were incubated at 37 °C for 20 min, washed once and re-suspended in the same NaCl Ringer bath solution. The Ca^{2+}-dependent fluorescence intensity was measured in fluorescence channel FL-1 in FACS analysis.

Where necessary, NA (100 nM, 100 μM, and 300 μM) or ethanol (for controls) was added to the NaCl Ringer bath solution during the loading of the cells with Fluo-3 in FACS analysis.

Electrophysiology

The patch-clamp recordings were performed at room temperature. Currents were recorded in fast whole-cell mode. The patch pipettes (1.5–3 M Ohm resistance) were made of borosilicate glass capillaries (150 TF-10, Clark Medical Instruments). Pipettes were connected via an Ag–AgCl wire to the head-stage of an EPC 9 patch-clamp amplifier (HEKA). Data acquisition and analysis were controlled by a computer equipped with ITC 16 interface (Instrutech) using Pulse software (HEKA). For current measurements, K562 cells were held at −10 mV holding potential (V_h) (Cl^- channel measurements) or 0 mM (SOC and SK4 channels measurements). The pulses (200 ms duration) from −100 to +100 mV were applied in increments of +20 mV. The applied voltages refer to the

cytoplasmic face of the membrane with respect to the extracellular space. The currents were analyzed by averaging the current values measured between 90 and 190 ms of each square pulse (I/V, current–voltage relationship) and corrected for the cell capacitance (7–16 pF).

The offset potentials between both electrodes were zeroed before sealing. The liquid junction potentials between bath and pipette solutions and between the bath solutions and the salt bridge (filled with NaCl bath solution) were calculated according to Barry and Lynch (1991).

NaCl Ringer bath solution used in our whole-cell patch-clamp experiments consisted of (in mM) 145 NaCl, 5 KCl, 2 $MgCl_2$, 1 $CaCl_2$, 5 glucose, and 10 HEPES (pH 7.4 with NaOH). The NMDG-aspartate (NMDG-Cl) bath solutions contained (in mM) 180 NMDG, 0 or 10 Ca-aspartate (or 1 $CaCl_2$), and 10 HEPES (pH 7.4 with aspartic acid or HCl).

Two types of pipette solutions were used for SOC channels measurements. The Na-aspartate (Na-Asp) and Cs-aspartate (Cs-Asp) pipette solutions consisted of (in mM) 140 Na-aspartate (120 Cs-aspartate), 10 NaCl (10 Cs-aspartate), 10 EGTA, and 10 HEPES (pH 7.4 with NaOH or CsOH). Tg (2 μM) was added to the Cs-Asp pipette solution. Ruthenium red (100 μM) dissolved in the Ca-containing NMDG-aspartate bath solution was added acutely.

Cl^- channels activity was estimated with the pipette solution contained (in mM) 180 NMDG, 1 MgATP, and 10 HEPES (pH 7.4 with aspartic acid). Tg (2 μM) and NA (100 and 300 μM) were dissolved in 1 mM $CaCl_2$-containing NMDG-Cl bath solution and added acutely.

SK4 channel activity was estimated with the highly Ca^{2+}-buffered pipette solution contained (in mM) 135 KCl, 6 NaCl, 0.5 $MgCl_2$, 3 MgATP, 10 EGTA, 0 or 8.4 $CaCl_2$ (8.71×10^{-7} M Ca^{2+} free), and 5 HEPES (pH 7.2 with NaOH). NA (100 and 300 μM) was dissolved in the NaCl Ringer bath solution and added acutely.

Reagents

Tg, ruthenium red, and NA were purchased from Sigma (Sigma, Germany). DMSO was used as a solvent for Tg stock solution (1 mM Tg), ethanol for NA.

Statistics

Data are expressed as arithmetic mean ± SEM and unpaired two-tailed *t* test was employed as appropriate, $p < 0.05$ was considered statistically significant.

Results

The micromolar (100 and 300 μM) concentrations of NA stimulated Annexin V binding in K562 cells (Fig. 1a, b). Lower (100 nM) concentration of NA was ineffective. The apoptotic effect of the micromolar NA concentrations was comparable with that of Tg, the ER mobilizing agent (Fig. 1a, c). Annexin V binding (Fig. 1c, d) was additionally enhanced in K562 cells upon combined NA and Tg treatment (Tg and NA, 24 h, +37 °C).

High micromolar (100–500 μM) NA concentrations are typically used for Ca^{2+}-activated Cl^- and Ca^{2+}-activated K^+ channels blockage (Astill et al. 1996; Liantonio et al. 2007; Chen et al. 2011; Ahn et al. 2004). To answer the question of possible involvement of Ca^{2+}-activated ion channels in apoptosis induced by NA (alone and in combination with Tg) the series of patch-clamp experiments were performed.

We first tested if CAC participate in the effect. When combined with NMDG-aspartate pipette, acute application of 1 mM $CaCl_2$ containing NMDG-Cl bath solution stimulated a strong outward current (Fig. 2b). Application of 2-μM Tg (Fig. 2c, g) significantly enhanced the current and shifted the reversal potential to more negative values (−47.6 ± 5.7 in the absence and −73.9 ± 3.0 mV in the presence of 2-μM Tg, respectively). Substitution of bath Cl^- with Asp^- completely abolished the current (Fig. 2d). Cl^- and CAC channels blocker NA and a selective TMEM16A channel blocker AO1 (De La Fuente et al. 2008; Davis et al. 2013) inhibited the outward current induced by Tg treatment (Fig. 2e, f). The current blockage was accompanied with a positive shift to −39.4 ± 4.0 mV within the first minutes of the CAC channels blockers application (Fig. 2e–g).

The CAC channels were not the only channels affected by NA in K562 cells. When recorded with Ca^{2+} (0.87 μM) containing KCl pipette solution, outwardly rectifying current developed in K562 cells within the first minutes of incubation (Fig. 3a, e). TMEM16A channel blocker AO1 (20 μM) blocked the outward current (Fig. 3b).

Acute application of NA inhibited, in time and concentration-dependent manner, outward Cl^- current and activated K^+ current. As it is shown in Fig. 3c, time required to induce outward current density of 16.85 ± 2.6 pA/pF at +100 mV was ~6 min for 300-μM NA and ~20 min for 100-μM NA. The cell hyperpolarization caused by NA was concentration-dependent (−38.2 ± 5.7 mV for 100-μM NA versus −54.1 ± 2.3 mV for 300-μM NA treatment, Fig. 3g).The I/V relationship with saturation at high positive potentials and a lack of voltage-dependency suggest that outward K^+ current stimulated by NA was due to SK4 channels. Indeed, a specific SK4 channels inhibitor TRAM-34 (1 μM) blocked the K^+ outward current induced by NA in K562 cells (Fig. 3d, f). In the absence of NA acute application of TRAM-34 restored the activity of CAC channels that resulted in a strong outward Cl^- current (Fig. 3d).

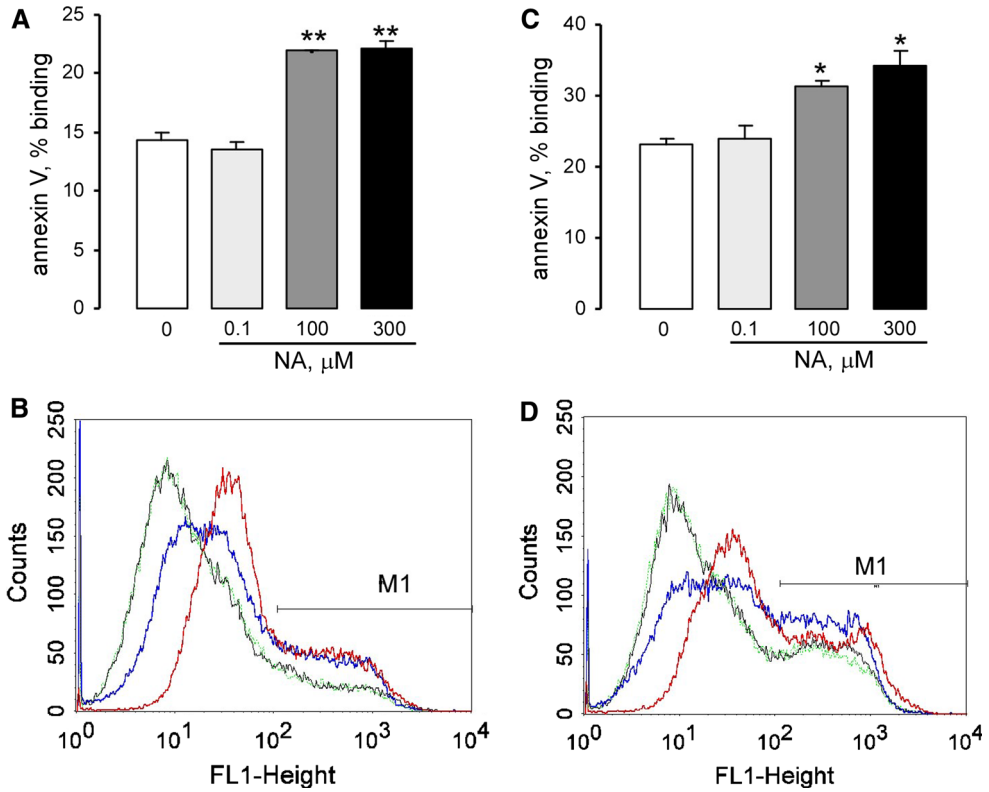

Fig. 1 Niflumic acid (NA) induced apoptosis in K562 cells. **a** Arithmetic mean ± SEM of Annexin V binding (%) in K562 cells incubated for 24 h with ethanol (*white bar*, $n = 5$), 100-nM NA (*light gray bar*, $n = 3$), 100-μM NA (*gray bar*, $n = 5$), and 300-μM NA (*black bar*, $n = 5$). *Double asterisks* indicate significant difference from control cells ($p < 0.01$; unpaired *t* test). **b** Histogram of Annexin V binding in a representative experiment on K562 cells in the absence (*black line*) or presence of 100-nM NA (*green line*), 100-μM NA (*blue line*), and 300-μM NA (*red line*), respectively. **c** Arithmetic mean ± SEM of normalized Annexin V binding (%) in K562 cells after 24 h incubation with 2-μM Tg in the absence (*white bar*, $n = 5$) and the presence of 100-nM NA (*light gray bar*, $n = 3$), 100 μM NA (*gray bar*, $n = 3$), and 300-μM NA (*black bar*, $n = 5$). *Asterisk* indicates significant difference from Tg-treated cells ($p < 0.05$, unpaired *t* test). **d** Histogram of Annexin V binding in a representative experiment with 2-μM Tg-treated K562 cells in the absence (*black line*) or presence of 100-nM NA (*green line*), 100-μM NA (*blue line*), and 300-μM NA (*red line*), respectively

Stimulation of SK4 channels leads to cell hyperpolarization and thus drives Ca^{2+} through Ca^{2+}-permeable channels. The main Ca^{2+} entry pathway in cancer cells is supported by "capacitive Ca^{2+} entry" activated by intracellular Ca^{2+} stores depletion. In the next series of experiments we tested the effect of NA on store-operated Ca^{2+}-permeable channels activity in K562 cells. To deplete Ca^{2+} stores in K562 cells, we utilized the highly (10 mM EGTA) Ca^{2+}-buffered Na-aspartate pipette solution.

When combined with Ca^{2+}-free NMDG-aspartate bath solution, a strong outward Na^+ current with the corresponding negative shift (−56.6 ± 2.7 mV) in the reversal potential (Fig. 4a, d) was induced. Addition of 10 mM $CaCl_2$ to the NMDG-aspartate bath solution (Fig. 4b, d) significantly blocked Na^+ outward current, increased inward (Ca^{2+}) current, and shifted the reversal potential to 15.08 ± 2.68 mV ($n = 6$). Acute application of NA significantly ($p < 0.001$) blocked inward Ca^{2+} current (Fig. 4c) and shifted the reversal potential to −2.5 ± 0.74 mV (Fig. 4d).

The channels permeability for Ca^{2+} over Na^+ measured in our experiments was $P_{Ca^{2+}}/P_{Na^+} = 16.78$ (Fig. 4d). High selectivity of Ca^{2+} over Na^+ and the absence of inward current when bath Ca^{2+} was substituted with Mg^{2+} suggest that the measured channels were store-operated Ca^{2+}-permeable channels. To prove that inward Ca^{2+} current in our experiments could be due to TRPV5/6 channels in K562 cells, we used a channel blocker ruthenium red (RR). Acute application of 100-μM RR inhibited a fraction of inward current in Ca^{2+}-containing bath solution (Fig. 4d). As it is seen in Fig. 4e, Ca^{2+} conductance was effectively blunted in the presence of RR as well as NA.

When I–V recordings were made with highly (10 mM EGTA) Ca^{2+}-buffered Cs-aspartate pipette solution reinforced with 2-μM Tg (see Fig. 5) the same blocking effect of NA on Ca^{2+} influx was observed. Noteworthy, NA (100

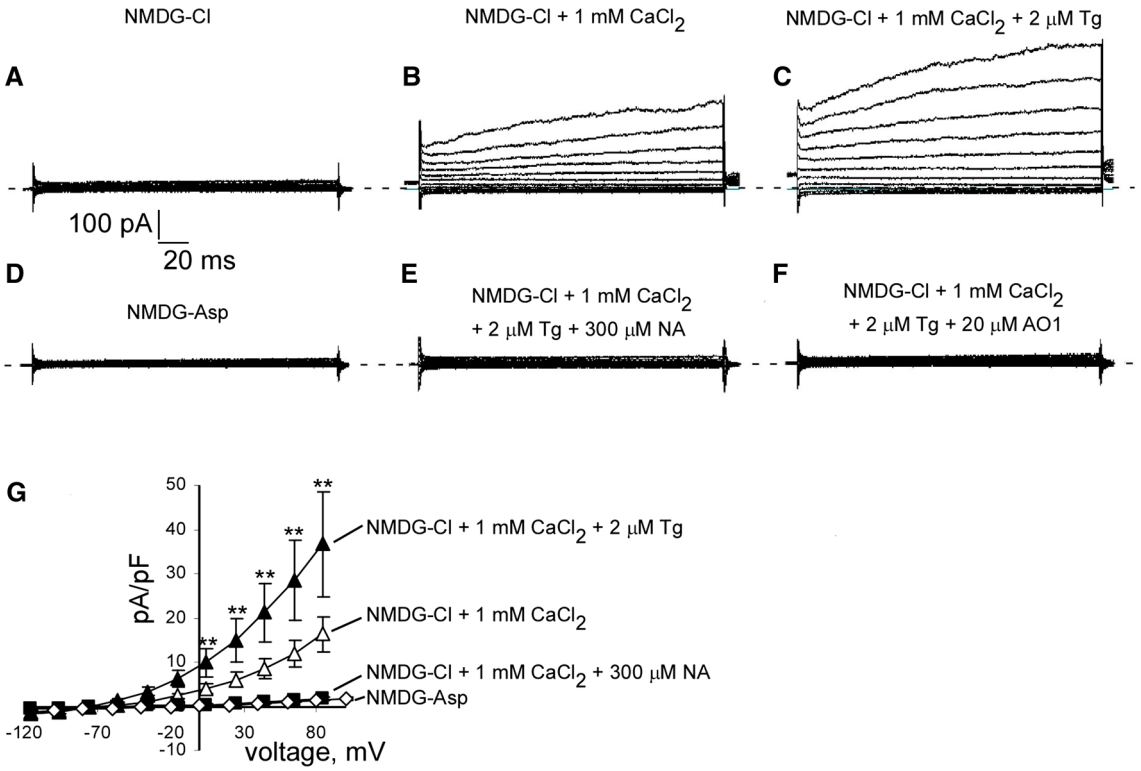

Fig. 2 NA blocks Cl^- current activated in K562 cells by intracellular free calcium ($[Ca^{2+}]_i$). **a** Whole-cell current tracings of K562 cells in 180 mM NMDG-Cl solution. **b** As in **a** for the cells in 180 mM NMDG-Cl bath solution supplemented with 1 mM $CaCl_2$ **c** as in **b** in the presence of 2-μM Tg in Ca^{2+}-containing NMDG-Cl bath solution **d** as in **a** for the cells suspended in 180 mM NMDG-aspartate solution **e** as in **c** in the presence of 300-μM NA **f** as in **c** in the presence of 20-μM AO1. **g** Arithmetic means (±SEM, $n = 5$) of the current as a function of voltage (*I/V* relationship), recorded with NMDG-aspartate pipette solution, in K562 cells suspended in NMDG-aspartate bath solution (*open diamonds*), 1 mM $CaCl_2$-containing NMDG-Cl bath solution (*open triangles*), the NMDG-Cl bath solution in the presence of 2-μM Tg (*closed triangles*) and the NMDG-Cl bath solution in the presence of 2-μM Tg and 300-μM NA (*closed squares*). *Double asterisks* indicate significant difference from the cells in the corresponding bath solution without Tg (paired $p \leq 0.01$)

and 300 μM) significantly blunted inward Ca^{2+} (Fig. 5d–f, h) and outward Cs^+ currents (Fig. 5a–c, g) suggesting the non-selective Ca^{2+}-permeable channels inhibition. Inhibitory effect of NA on Ca^{2+} influxes was concentration-dependent. The nanomolar concentration of NA (100 nM; IC_{50} for COX-2 inhibition) reduced Ca^{2+} permeability of the channels ($P_{Ca^{2+}}/P_{Cs^+} = 2.57$ in absence and $P_{Ca^{2+}}/P_{Cs^+} = 1.5$ in the presence of 100 nM NA), however, it did not affect Ca^{2+} conductance of the channels as it is shown in Fig. 5i. Acute application of the micromolar (μM) NA concentrations additionally reduced Ca^{2+} permeability of the channels ($P_{Ca^{2+}}/P_{Cs^+} = 0.91$ for 100 μM and $P_{Ca^{2+}}/P_{Cs^+} = 0.9$ for 300-μM NA, respectively) and blunted Ca^{2+} conductance (the effect was significant at 300-μM NA, Fig. 5i).

The FACs experiments with Fluo-3 further confirmed the blocking effect of the micromolar NA concentrations on store-operated Ca^{2+} influx in K562 cells. As it is shown in Fig. 6, 100 nM NA had no effect on $[Ca^{2+}]_i$ in K562 cells in the presence and the absence of Tg. In contrary, $[Ca^{2+}]_i$ was blunted in the 100 and 300 μM of NA-treated cells. Noteworthy, NA-treated K562 cells showed the same as control untreated cells intracellular Ca^{2+} levels when NA was removed from the bath medium during Fluo-3 loading procedure (see Fig. 6e).

The apoptotic and Ca^{2+} blocking effects of NA in K562 cells were then compared with the effects of 2-APB, a SOC channels inhibitor. In our experiments, incubation of K562 cells either with 100-μM NA or 100-μM 2-APB resulted in a significant decline in $[Ca^{2+}]_i$ and enhanced cell apoptosis (see Fig. 7).

Thus, we show that NA regulation of Ca^{2+}-activated (Cl^- and K^+) and Ca^{2+}-permeable (store-operated) ion channels contributed to NA-stimulated apoptosis in K562 cells.

Discussion

NA belongs to a NSAID group that shows COX-2 inhibitory activity. COX-2 is up-regulated in a number of cancer cells that stimulates excessive prostaglandins (mainly

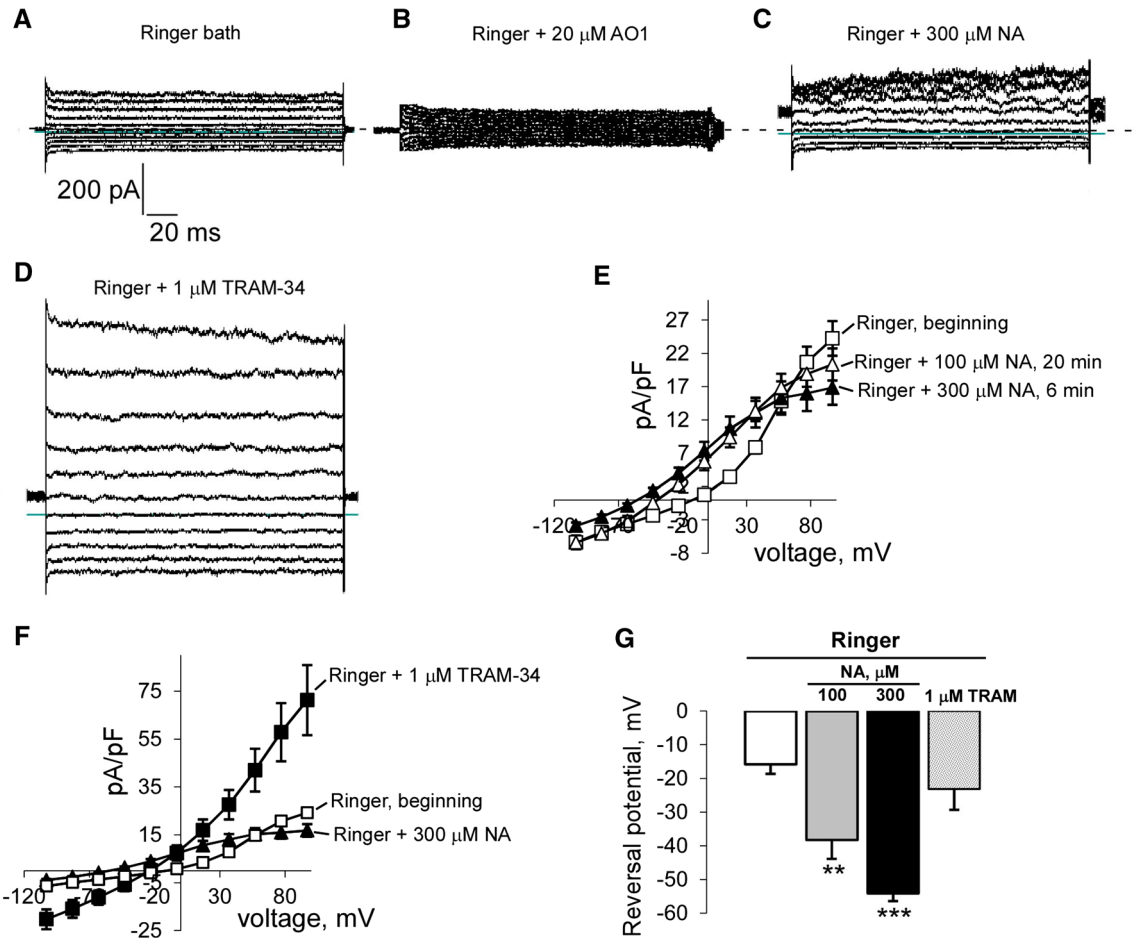

Fig. 3 NA activates SK4 channels in K562 cells. **a** Whole-cell current tracings recorded with Ca^{2+}-containing (0.87-μM Ca^{2+} free) KCl pipette solution in K562 cells in NaCl Ringer bath solution. **b** As in **a** after acute application of 20-μM AO1. **c** As in **a** after acute application of 300-μM NA. **d** As in **c** after acute application of 1-μM TRAM-34. **e** Arithmetic means (±SEM) of the current as a function of voltage (I/V relationship) in K562 cells in NaCl Ringer bath solution in the absence (*open squares*, $n = 13$), and after acute application of 100-μM NA (*open triangles*, $n = 5$) and 300-μM NA (*closed triangles*, $n = 13$). **f** Arithmetic means (±SEM) of the current as a function of voltage (I/V relationship) in K562 cells in NaCl Ringer bath solution (*open squares*, $n = 13$) acutely stimulated with 300-μM NA (*closed triangles*, $n = 13$) and then exposed to 1-μM TRAM-34 (*closed squares*, $n = 6$). **g** Reversal potential (mV, ±SEM) calculated from the original I/V relationships in K562 cells under the control conditions (*open bar*, $n = 13$), in the cells acutely stimulated with 100-μM NA (*gray bar*, $n = 5$) and 300-μM NA (*black bar*, $n = 13$) followed by 1-μM TRAM-34 exposure (*dotted bar*, $n = 6$)

PGE_2) production. PGE_2 is known to enhance tumor cell growth. However, a direct involvement of COX-2 in apoptotic effect of NSAIDs is not well proved. PGE_2 was reported to induce apoptosis in K562 cells (Föller et al. 2006). While the literature data concerning NA effect on haematopoietic cancer cells are missing, other specific COX-2 inhibitors (nimesulide, NS-398, celecoxib) were shown to induce apoptosis of chronic myeloid leukemia cells (Cerella et al. 2011; Subhashini et al. 2005; Zhang et al. 2006) via COX-2 independent mechanism (Cerella et al. 2011).

We have demonstrated here that NA (100 and 300 μM) induced apoptosis and enhanced Tg-induced apoptosis in K562 cells when used in concentrations much higher than that for IC_{50} COX-2 inhibition (100 nM). It suggests COX-2 independent mechanism of NA-stimulated apoptosis in K562 cells.

Instead, apoptotic effect of NA in K562 cells could be due to ion channel modulation by NA. Increasing number of publications show that ion channels play a significant role in cancer cells metabolism and may help to determine the typical features of cancer cells, such as independence of mitogenic and antimitogenic signals, avoidance of apoptosis, indefinite proliferative potential, and capability of inducing angiogenesis (Becchetti 2011; Prevarskaya et al. 2011).

NA is known to modulate the activity of a number of channels including Cl^- and CAC (Astill et al. 1996;

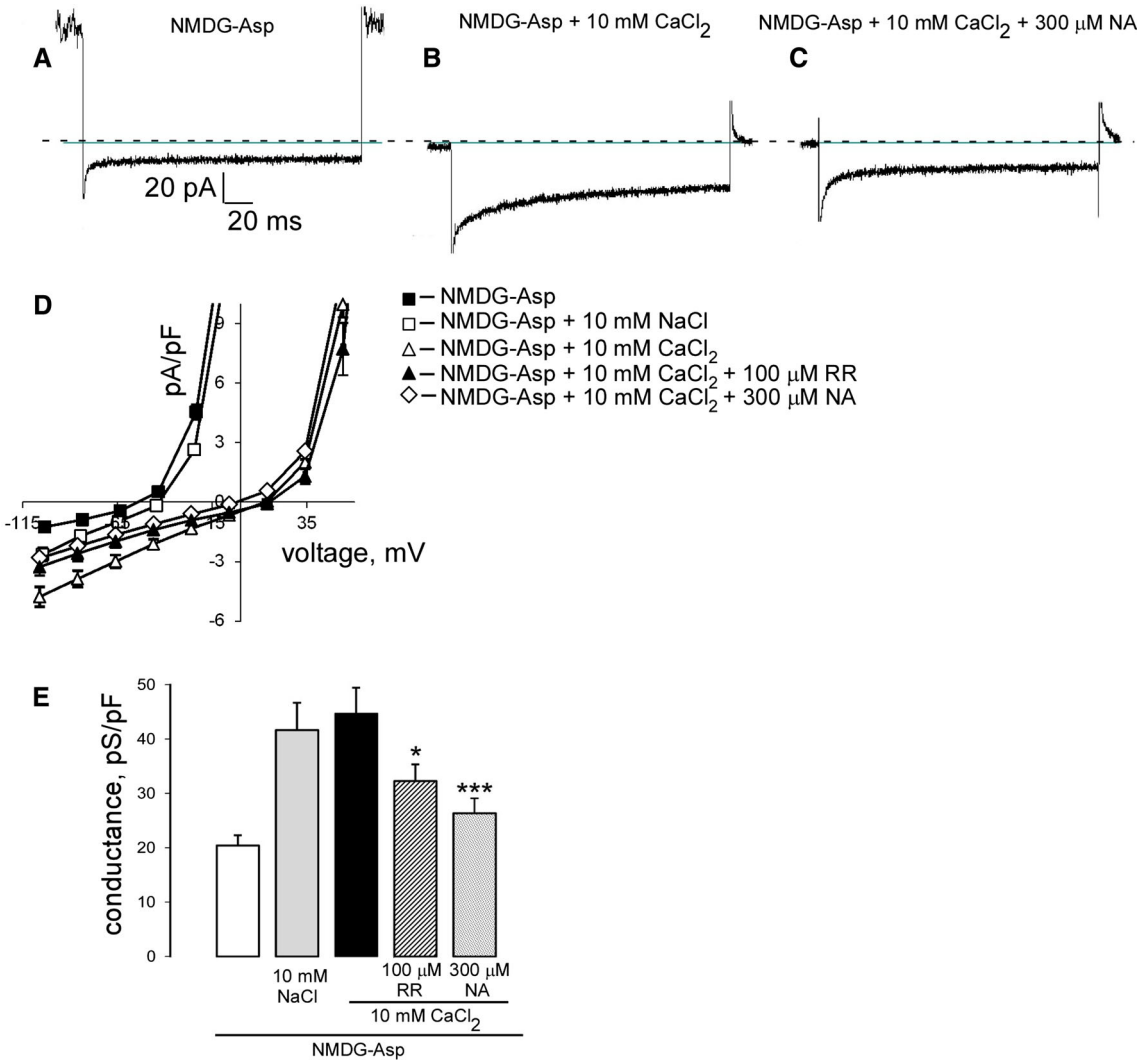

Fig. 4 Acute application of NA blunts Ca^{2+} current in K562 cells. **a** Current tracing, recorded with 10 mM EGTA containing Na-aspartate pipette solution at −100 mV, in K562 cells suspended in Ca^{2+}-free 180 mM NMDG-aspartate bath solution. **b** As in **a** after acute application of 10 mM $CaCl_2$. **c** As in **b** in the presence of 300-μM NA. **d** Arithmetic means of I–V relationships (±SEM, $n = 7$), recorded with high (10 mM EGTA) Ca^{2+} buffered Na-aspartate pipette solution, in K562 cells suspended in Ca^{2+}-free NNDG-aspartate bath solution (*closed squares*), 10 mM NaCl containing NMDG-aspartate bath solution (*open squares*), 10 mM $CaCl_2$ containing NMDG-aspartate bath solution (*open triangles*) in the presence of 300-μM NA (*open diamonds*) or ruthenium red (*closed triangles*). **e** Arithmetic means (±SEM, $n = 7$) of the conductance (as calculated for the inward currents by linear regression) in K562 cells in Ca^{2+}-free NNDG-aspartate bath solution (*white bar*); 10 mM NaCl containing NMDG-aspartate bath solution (*gray bar*); 10 mM $CaCl_2$ containing NMDG-aspartate bath solution (*black bar*) in the presence of 100-μM ruthenium red (*striped bar*) or 300-μM NA (*dotted bar*). *Double asterisks* and *triple asterisks* indicate significant differences from the cells in 10 mM $CaCl_2$ containing NMDG-aspartate bath solution (paired *t* test $p \leq 0.01$ and $p \leq 0.001$, respectively)

Wangemann et al. 1986; Liantonio et al. 2006; Chen et al. 2011; Pifferi et al. 2006); large- (BK_{Ca}) and intermediate-conductance Ca^{2+}-activated K^+ channels (Li et al. 2008a; Ahn et al. 2004); ryanodine-sensitive Ca^{2+} release channels (Li et al. 2008b).

Since proliferation and tumor cells growth require persistently increased $[Ca^{2+}]_i$ and Ca^{2+} entry in cancer cells is operated mainly via specialized plasma membrane store-operated Ca^{2+}-permeable channels (SOC), we assumed that apoptotic effect of NA could be due to SOC channels modulation in K562 cells.

K562 cells were shown to express several SOC channels: TRPV5/6 (Semenova et al. 2009), formyl-peptide receptor like 1 CRAC channels (Li et al. 2008a, b, c), and TRPC3 (Föller et al. 2006). In our patch-clamp experiments, we utilized two types of highly Ca^{2+}-buffered pipette solutions: Na-aspartate pipette solution designed for TRPV5/6 channels measurements (Lee et al. 2005) and Cs-

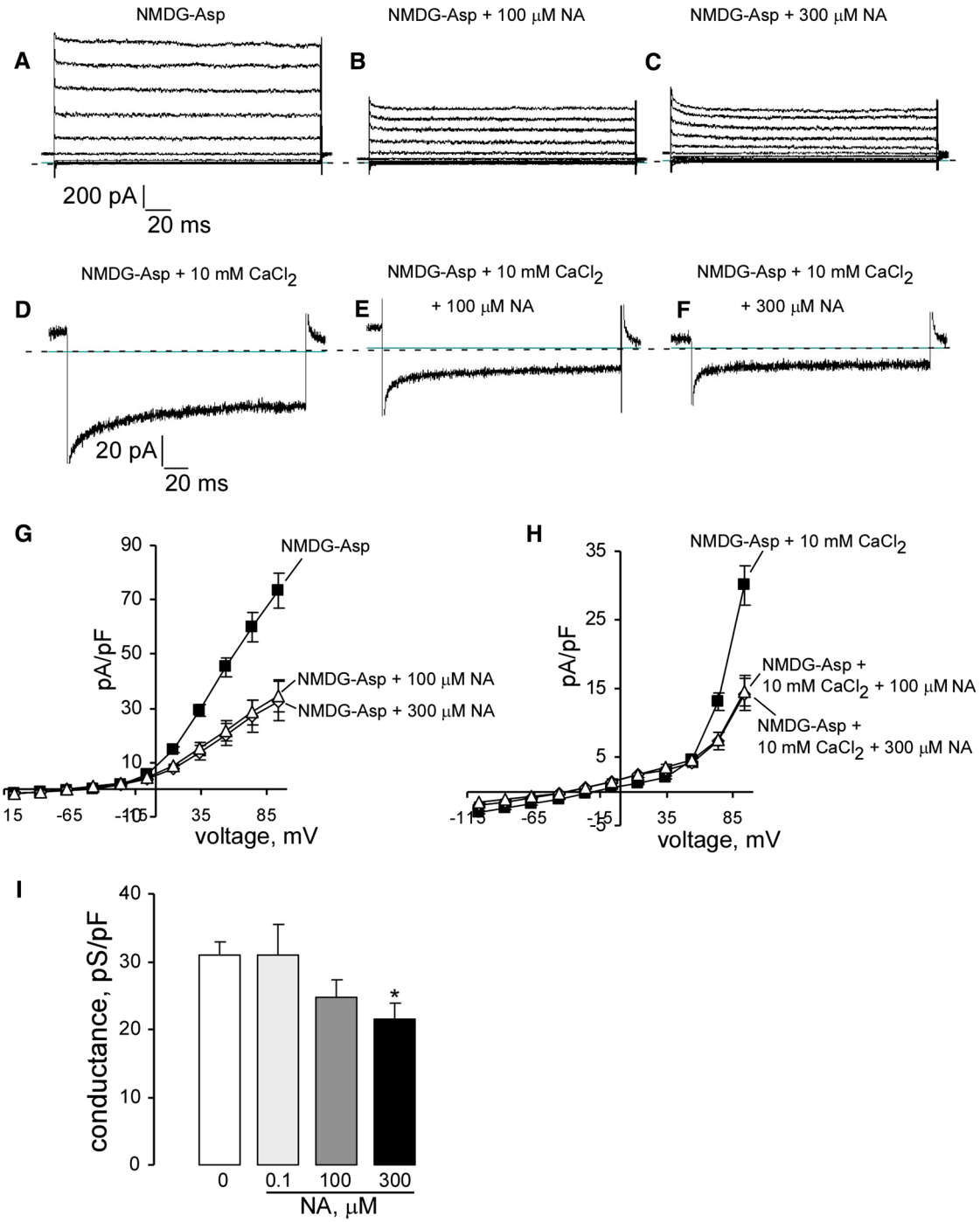

Fig. 5 NA inhibits store-operated Ca^{2+} channels in K562 cells. **a** Whole-cell current tracings, recorded with 10 mM EGTA containing Cs-aspartate pipette solution, in K562 cells suspended in Ca^{2+}-free180 mM NMDG-aspartate bath solution. **b** As in **a** after acute application of 100-μM NA dissolved in NMDG-aspartate bath solution. **c** As in **b** after acute application of 300-μM NA dissolved in NMDG-aspartate bath solution. **d** Current tracing recorded at −100 mV in K562 cells suspended in 10 mM $CaCl_2$ containing 180 mM NMDG-aspartate bath solution. **e** As in **d** in the presence of 100-μM NA. **f** As in **d** in the presence of 300-μM NA. **g** Arithmetic means of I–V relationships (±SEM, $n = 7$–15), recorded with highly Ca^{2+} buffered Cs-aspartate pipette solution, in K562 cells suspended in Ca^{2+}-free NNDG-aspartate bath solution in the absence (*closed squares*) and presence of 100-μM NA (*open triangles*) or 300-μM NA (*open diamonds*). **h** Arithmetic means of I–V relationships (±SEM, $n = 7$–15), recorded with highly Ca^{2+} buffered Cs-aspartate pipette solution, in K562 cells suspended in 10 mM $CaCl_2$ containing NNDG-aspartate bath solution in the absence (*closed squares*) and presence of 100-μM NA (*open triangles*) or 300-μM NA (*open diamonds*). **i** Arithmetic means (±SEM, $n = 7$–15) of the conductance (as calculated for the inward currents by linear regression) in K562 cells in 10 mM $CaCl_2$ containing NNDG-aspartate bath solution in the absence (*white bar*) and presence of 100-nM NA, 100 and 300 μM (*light gray*, *gray* and *black bars*, respectively). *Asterisk* indicates significant difference from control (paired *t* test $p \leq 0.05$)

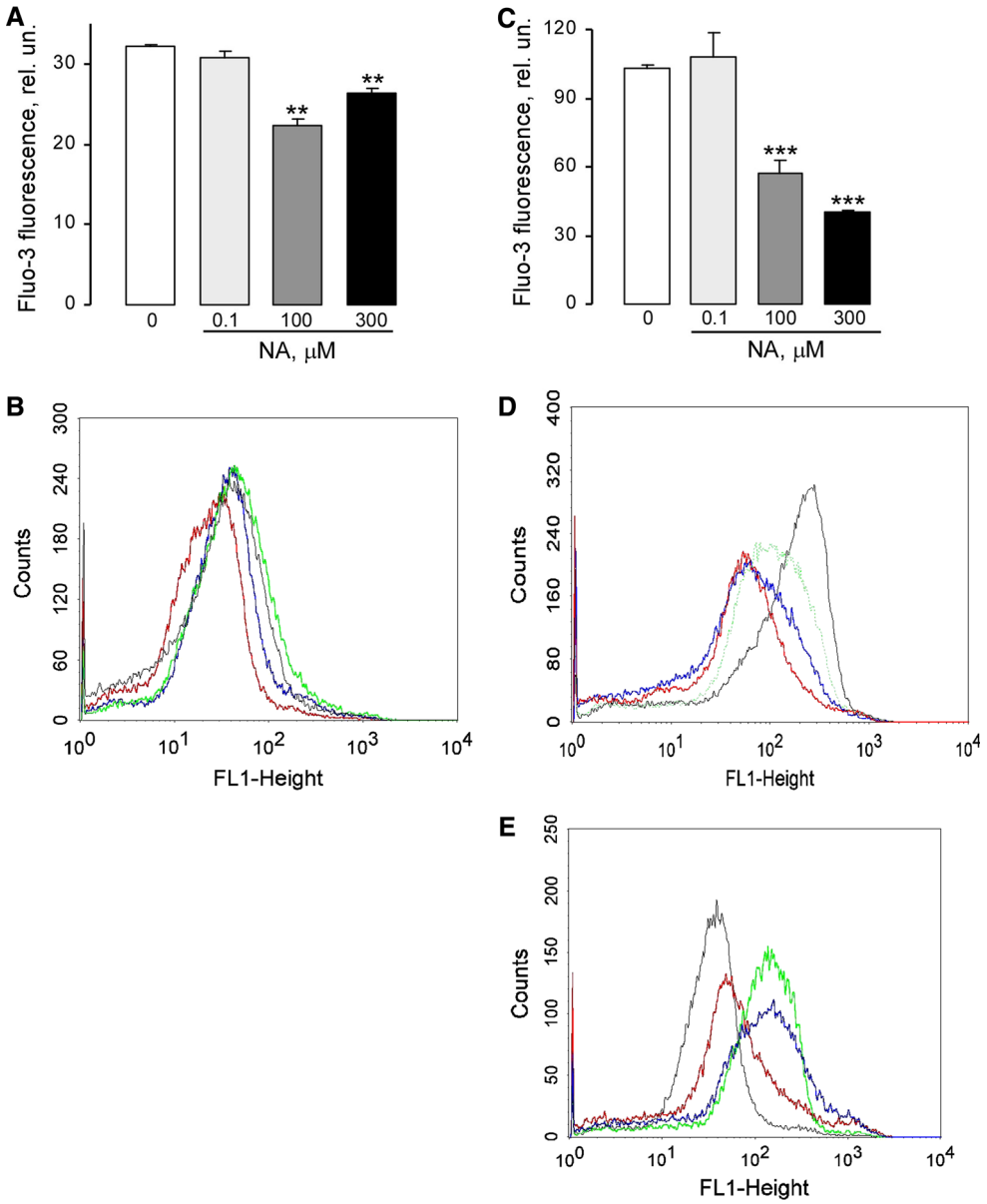

Fig. 6 NA reduced $[Ca^{2+}]_i$ in control and Tg-treated K562 cells. **a** Arithmetic mean ± SEM of Fluo-3 fluorescence of K562 cells incubated for 24 h in the absence (*white bar*, $n = 5$) and presence of 100-nM NA (*light gray bar*, $n = 3$), 100-μM NA (*gray bar*, $n = 3$) or 300-μM NA (*black bar*, $n = 5$). *Triple asterisks* indicate significant difference from control cells in the absence of NA ($p < 0.001$). **b** Histogram of Fluo-3 fluorescence in a representative experiment on K562 cells incubated for 24 h in the absence (*black line*), or presence of 100-nM NA (*green line*), 100-μM NA (*blue line*), and 300-μM NA (*red line*), respectively. **c** Arithmetic mean ± SEM of Fluo-3 fluorescence of K562 cells incubated with 2-μM Tg for 24 h in the absence (*white bar*, $n = 6$) and presence of 100-nM NA (*light gray bar*, $n = 3$), 100-μM NA (*gray bar*, $n = 3$), or 300-μM NA (*black bar*, $n = 6$). *Triple asterisks* indicate significant difference from Tg-treated cells ($p < 0.001$, unpaired t test). **d** Histogram of Fluo-3 fluorescence in a representative experiment with 2-μM Tg-treated K562 cells in the absence (*black line*), or presence of 100-nM NA (*green line*), 100-μM NA (*blue line*), and 300-μM NA (*red line*), respectively. **e** Histogram of Fluo-3 fluorescence in a representative experiment with K562 cells incubated for 24 h with 300-μM NA in the absence (*black* and *red lines*) and presence of 2-μM Tg (*green* and *blue lines*). NA was present (*black* and *green lines*) or removed from the Fluo-3 loading bath (*red* and *blue lines*), respectively

aspartate used for CRAC channels recordings (Huang and Ye 2008). The pipette solutions did not contain Mg^{2+} since Mg^{2+} was reported to induce a fast and voltage-dependent block and a slower inhibition of TRPV5 channels (Lee et al. 2005). However, lack of intracellular Mg^{2+} might promote ubiquitously expressed non-selective TRPM7 cation channels activation (Monteilh-Zoller et al. 2003; Sun et al. 2013). The principal difference between TRPM7

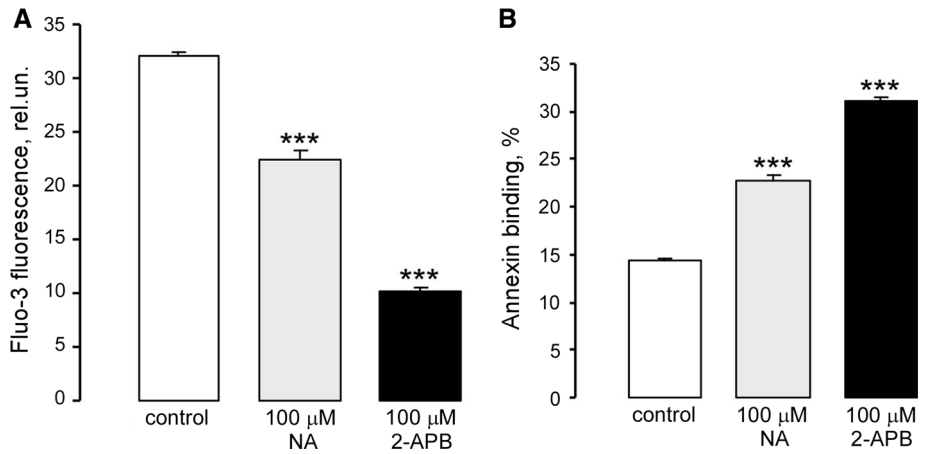

Fig. 7 Effects of 2-ABP and NA on apoptosis and $[Ca^{2+}]_i$. **a** Arithmetic mean ± SEM of Fluo-3 fluorescence in K562 cells incubated for 24 h with ethanol (*white bar*, $n = 10$), 100-μM NA (*light gray bar*, $n = 10$), 100-μM 2-APB (*black bar*, $n = 8$). *Triple asterisks* indicate significant difference from control cells ($p < 0.001$; unpaired *t* test). **b** Arithmetic mean ± SEM of Annexin V binding (%) in K562 cells incubated for 24 h with ethanol (*white bar*, $n = 10$), 100-μM NA (*light gray bar*, $n = 10$), 100-μM 2-APB (*black bar*, $n = 6$). *Triple asterisks* indicate significant difference from control cells ($p < 0.001$; unpaired *t* test)

and CRAC (or TRPV5/6) channels is the channel permselectivity. TRPM7 channels are Mg^{2+}-conducting channels with the permeability sequence: $K^+ > Cs^+ \sim Na^+ > Ca^{2+}$ (Runnels et al. 2001). In opposite to TRPM7 channels, CRAC and TRPV5/6 channels are highly selective Ca^{2+}-conducting channels. In our patch-clamp experiments substitution of bath Ca^{2+} with Mg^{2+} did not induce inward cation current. The channels permeability for Ca^{2+} over Na^+ measured in our experiments was $P_{Ca^{2+}}/P_{Na^+} = 16.78$. Moreover, acute application of ruthenium red, a blocker of TRPV5/6 but not TRPM7 channels, inhibited a fraction of inward current in Ca^{2+}-containing bath solution. Thus, we concluded that the I–V recordings made in the absence of intracellular Mg^{2+} indeed present store-operated Ca^{2+}-permeable channels in K562 cells.

Our data demonstrated a decline in the basal Ca^{2+} influx via SOC channels upon acute NA treatment. Noteworthy, we found no difference between 1 day NA-treated K562 cells and control untreated cells when NA was removed from the incubation medium during Fluo-3 loading procedure of 20 min. It suggests that the mechanism of the channels inhibition by NA is reversible and permanent presence of NA is necessary for the channels blockage.

The recent study demonstrated that pharmacological inhibition of SOC channels with SKF-96365 or 2-APB increased apoptosis of C-6 glioblastoma cell line (Liu et al. 2011). Our experiments showed that both 2-APB (100 μM), a SOC and human TRPV6 channels inhibitor (Kovacs et al. 2012), and NA (100 μM) induced apoptosis and blunted $[Ca^{2+}]_i$ in K562 cells. Thus, we assumed that blockage of SOC channels by NA could be the main mechanism for apoptotic effect of NA in K562 cells.

Interestingly, the percentage of apoptosis induced by NA treatment was comparable with that induced by the SR Ca^{2+} pump blocker Tg. Combined treatment of the cells with NA and Tg enhanced apoptotic levels in K562 cells.

Tg was shown to act as a tumor promoter stimulating Src tyrosine kinase that in turn activates Raf-1 and MAP kinase (Chao et al. 1997). At the same time Tg induces apoptosis through activation of ER stress and Ca^{2+} entry pathways. In combination with a targeting peptide, that is, a substrate of the serine/protease prostate-specific antigen, Tg is used for developing cell-specific prodrugs (also known as "smart bomb") (Denmeade and Isaacs 2005). Mechanism of Tg-induced apoptosis in K562 cells involves ER stress, cleavage, and activation of caspase-3, -7, -9, -12, disruption of the mitochondrial membrane potential and cytochrome C release (Feng et al. 2006).

Tg treatment induces Ca^{2+} release from ER stores that in turn may stimulate Ca^{2+}-activated channels. Literature data indicate that Ca^{2+}-activated Cl^- and Ca^{2+}-activated K^+ channels play a central role in tumor cells survival. Activation of SK4 channels was shown to enhance apoptosis in K562 cells (Lang et al. 2003). Enhanced level of $[Ca^{2+}]_i$, upon cyclosporin A application, induced Cl^- efflux and resulted in a dose- and time-dependent apoptosis in human hepatoma cells (Kim et al. 2003).

Acute application of Tg induced outward Cl^- current in our patch-clamp experiments. The current was strongly inhibited by NA and AO1, a selective TMEM16A Ca^{2+}-activated channel blocker. We also consider a possibility of Ca^{2+}-dependent kinases participation in Cl^- conductance activation. CAC are known to be calmodulin regulated (Kaneko et al. 2006). As for TMEM16A CAC, it was shown that both cGMP-dependent and independent

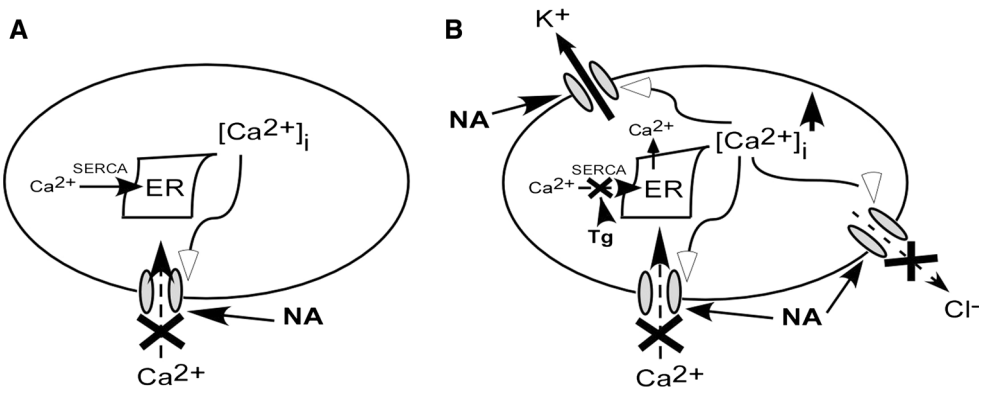

Fig. 8 Schematic representation of NA effects on ion channels activity leading to apoptosis in K562 cells. **a** Apoptosis in NA-treated K562 cells is connected with SOC channels inhibition. **b** SOC and CAC inhibition and Ca^{2+}-activated K^+ channel activation by NA result in enhanced K562 cells apoptosis upon combined NA and Tg treatment

components are involved in the channels Cl^- conductance (Dam et al. 2013).

Interestingly, inhibition of CAC channels by NA in our patch-clamp experiments was accompanied by activation of K^+ outward currents in time and concentration-dependent manner. In Ca^{2+}-containing KCl pipette solution, the outward current at the beginning of experiment related to Ca^{2+}-dependent Cl^- conductance (CAC channels) since it was blocked by the TMEM 16A channel inhibitor AO1. Activation of SK4 channel requires higher cytosolic free Ca^{2+} levels ($\sim$4.7 μM). The biophysical characteristics of the outward current induced by NA and its blockage by TRAM-34 suggest the SK4 channels activation in K562 cells. Thus, our data confirmed the previously reported data (Ahn et al. 2004) showing that NA increases sensitivity of SK4 channels to cytosolic Ca^{2+}.

In conclusion, our data suggest that mechanism of NA-induced apoptosis in K562 cells is COX-2 independent. The micromolar concentrations of NA are required for the cells apoptosis. Inhibition of SOC channels plays a major role in NA-induced apoptosis (Fig. 8a). Increased apoptotic levels in Tg-treated K562 cells in the presence of NA may be due to the blockage of Ca^{2+}-activated Cl^- and stimulation of Ca^{2+}-activated K^+ (SK4) channels (see Fig. 8b) in addition to SOC channels inhibition.

NA was the only NSAID of fenamate group used in the study. The most recent data have shown that the members of fenamate group and Cl^- channels inhibitors NA and flufenamic acid had the similar potentiation effects on BK_{Ca} channel activity in the arteriolar smooth muscle cells (Li et al. 2013). Fenamates were also reported to inhibit TRPC4/TRPC5 (Jiang et al. 2012), TRPM2 channels (Chen et al. 2012) and activate $[Na^+]_i$-regulated human Slo2.1 channels (Garg and Sanguinetti 2012). Whether other members of the group have similar to NA pro-apoptotic effects in erythroleukemic K562 cells could be a subject of further studies.

Acknowledgments The experiments were carried out in Physiological Department I University of Tuebingen, Germany. Y. V. K. thanks the Head of Physiological Department I Prof. Dr. Florian Lang for the post-doctoral fellowship. Y. V. K. thanks Mr. David Andrew Erickson (Phoenix, USA) for correcting the final version of the manuscript.

References

Ahn SC, Seol GH, Kim JA, Suh SH (2004) Characteristics and a functional implication of Ca(2+)-activated K(+) current in mouse aortic endothelial cells. Pflugers Arch 447(4):426–435

Astill DS, Rychkov G, Clarke JD, Hughes BP, Roberts ML, Bretag AH (1996) Characteristics of skeletal muscle chloride channel C1C-1 and point mutant R304E expressed in Sf-9 insect cells. Biochim Biophys Acta 1280(2):178–186

Barry PH, Lynch JW (1991) Liquid junction potentials and small cell effects in patch-clamp analysis. J Membr Biol 121(2):101–117

Becchetti A (2011) Ion channels and transporters in cancer. 1. Ion channels and cell proliferation in cancer. Am J Physiol Cell Physiol 301(2):C255–C265

Cao Y, Prescott SM (2002) Many actions of cyclooxygenase-2 in cellular dynamics and in cancer. J Cell Physiol 190(3):279–286

Cerella C, Sobolewski C, Chateauvieux S, Henry E, Schnekenburger M, Ghelfi J, Dicato M, Diederich M (2011) COX-2 inhibitors block chemotherapeutic agent-induced apoptosis prior to commitment in hematopoietic cancer cells. Biochem Pharmacol 82(10):1277–1290

Chao TS, Abe M, Hershenson MB, Gomes I, Rosner MR (1997) Src tyrosine kinase mediates stimulation of Raf-1 and mitogen-activated protein kinase by the tumor promoter thapsigargin. Cancer Res 57(15):3168–3173

Chen Y, An H, Li T, Liu Y, Gao C, Guo P, Zhang H, Zhan Y (2011) Direct or indirect regulation of calcium-activated chloride channel by calcium. J Membr Biol 240(3):121–129

Chen GL, Zeng B, Eastmond S, Elsenussi SE, Boa AN, Xu SZ (2012) Pharmacological comparison of novel synthetic fenamate analogues with econazole and 2-APB on the inhibition of TRPM2 channels. Br J Pharmacol 167(6):1232–1243

Dam VS, Boedtkjer DM, Nyvad J, Aalkjaer C, Matchkov V (2013) TMEM16A knockdown abrogates two different Ca(2+)-activated Cl(−) currents and contractility of smooth muscle in rat mesenteric small arteries. Pflugers Arch (in print)

Davis AJ, Shi J, Pritchard HA, Chadha PS, Leblanc N, Vasilikostas G, Yao Z, Verkman AS, Albert AP, Greenwood IA (2013) Potent vasorelaxant activity of the TMEM16A inhibitor T16A(inh)-A01. Br J Pharmacol 168(3):773–784

De La Fuente R, Namkung W, Mills A, Verkman AS (2008) Small-molecule screen identifies inhibitors of a human intestinal

calcium-activated chloride channel. Mol Pharmacol 73(3):758–768

Denmeade SR, Isaacs JT (2005) The SERCA pump as a therapeutic target: making a "smart bomb" for prostate cancer. Cancer Biol Ther 4(1):14–22

Feng XQ, You Y, Xiao J, Zou P (2006) Thapsigargin-induced apoptosis of K562 cells and its mechanism. Zhongguo Shi Yan Xue Ye Xue Za Zhi 14(1):25–30

Föller M, Kasinathan RS, Duranton C, Wieder T, Huber SM, Lang F (2006) PGE2-induced apoptotic cell death in K562 human leukaemia cells. Cell Physiol Biochem 17(5–6):201–210

Garg P, Sanguinetti MC (2012) Structure-activity relationship of fenamates as Slo2.1 channel activators. Mol Pharmacol 82(5):795–802

Huang YP, Ye DY (2008) Formyl-peptide receptor like 1: a potent mediator of the Ca^{2+} release-activated Ca^{2+} current ICRAC. Arch Biochem Biophys 478(1):110–118

Jiang H, Zeng B, Chen GL, Bot D, Eastmond S, Elsenussi SE, Atkin SL, Boa AN, Xu SZ (2012) Effect of non-steroidal anti-inflammatory drugs and new fenamate analogues on TRPC4 and TRPC5 channels. Biochem Pharmacol 83(7):923–931

Kaneko H, Möhrlen F, Frings S (2006) Calmodulin contributes to gating control in olfactory calcium-activated chloride channels. J Gen Physiol 127(6):737–748

Kim JA, Kang YS, Lee YS (2003) Role of Ca^{2+}-activated Cl-channels in the mechanism of apoptosis induced by cyclosporin A in a human hepatoma cell line. Biochem Biophys Res Commun 309(2):291–297

Kim BM, Maeng K, Lee KH, Hong SH (2011) Combined treatment with the Cox-2 inhibitor niflumic acid and PPARÎ³ ligand ciglitazone induces ER stress/caspase-8-mediated apoptosis in human lung cancer cells. Cancer Lett 300(2):134–144

Kovacs G, Montalbetti N, Simonin A, Danko T, Balazs B, Zsembery A, Hediger MA (2012) Inhibition of the human epithelial calcium channel TRPV6 by 2-aminoethoxydiphenylborate (2-APB). Cell Calcium 52(6):468–480

Lang PA, Kaiser S, Myssina S, Wieder T, Lang F, Huber SM (2003) Role of Ca^{2+}-activated K^+ channels in human erythrocyte apoptosis. Am J Physiol Cell Physiol 285(6):C1553–C1560

Lee J, Cha SK, Sun TJ, Huang CL (2005) PIP2 activates TRPV5 and releases its inhibition by intracellular Mg^{2+}. J Gen Physiol 126(5):439–451

Li L, Ma KT, Zhao L, Si JQ, Zhang ZS, Zhu H, Li J (2008a) Niflumic acid hyperpolarizes smooth muscle cells via calcium-activated potassium channel in spiral modiolar artery of guinea pigs. Acta Pharmacol Sin 29(7):789–799

Li L, Ma KT, Zhao L, Si JQ (2008b) Niflumic acid hyperpolarizes the smooth muscle cells by opening BK(Ca) channels through ryanodine-sensitive Ca(2+) release in spiral modiolar artery. Sheng Li Xue Bao 60(6):743–750

Li YS, Wu P, Zhou XY, Chen JG, Cai L, Wang F, Xu LM, Zhang XL, Chen Y, Liu SJ, Huang YP, Ye DY (2008c) Formyl-peptide receptor like 1: a potent mediator of the Ca^{2+} release-activated Ca^{2+} current ICRAC. Arch Biochem Biophys 478(1):110–118

Li XZ, Ma KT, Guan BC, Li L, Zhao L, Zhang ZS, Si JQ, Jiang ZG (2013) Fenamates block gap junction coupling and potentiate BKCa channels in guinea pig arteriolar cells. Eur J Pharmacol 703(1–3):74–82

Liantonio A, Picollo A, Babini E, Carbonara G, Fracchiolla G, Loiodice F, Tortorella V, Pusch M, Camerino DC (2006) Activation and inhibition of kidney CLC-K chloride channels by fenamates. Mol Pharmacol 69(1):165–173

Liantonio A, Giannuzzi V, Picollo A, Babini E, Pusch M, Conte Camerino D (2007) Niflumic acid inhibits chloride conductance of rat skeletal muscle by directly inhibiting the CLC-1 channel and by increasing intracellular calcium. Br J Pharmacol 150(2):235–247

Liu H, Hughes JD, Rollins S, Chen B, Perkins E (2011) Calcium entry via ORAI1 regulates glioblastoma cell proliferation and apoptosis. Exp Mol Pathol 91(3):753–760

Monteilh-Zoller MK, Hermosura MC, Nadler MJ, Scharenberg AM, Penner R, Fleig A (2003) TRPM7 provides an ion channel mechanism for cellular entry of trace metal ions. J Gen Physiol 121(1):49–60

Pifferi S, Pascarella G, Boccaccio A, Mazzatenta A, Gustincich S, Menini A, Zucchelli S (2006) Bestrophin-2 is a candidate calcium-activated chloride channel involved in olfactory transduction. Proc Natl Acad Sci USA 103(34):12929–12934

Poronnik P, Ward MC, Cook DI (1992) Intracellular Ca^{2+} release by flufenamic acid and other blockers of the non-selective cation channel. FEBS Lett 296(3):245–248

Prevarskaya N, Skryma R, Shuba Y (2011) Calcium in tumour metastasis: new roles for known actors. Nat Rev Cancer 11(8):609–618

Runnels LW, Yue L, Clapham DE (2001) TRP-PLIK, a bifunctional protein with kinase and ion channel activities. Science 291(5506):1043–1047

Semenova SB, Vassilieva IO, Fomina AF, Runov AL, Negulyaev YA (2009) Endogenous expression of TRPV5 and TRPV6 calcium channels in human leukemia K562 cells. Am J Physiol Cell Physiol 296(5):C1098–C1104

Subhashini J, Mahipal SV, Reddanna P (2005) Anti-proliferative and apoptotic effects of celecoxib on human chronic myeloid leukemia in vitro. Cancer Lett 224(1):31–43

Sun Y, Selvaraj S, Varma A, Derry S, Sahmoun AE, Singh BB (2013) Increase in serum Ca^{2+}/Mg^{2+} ratio promotes proliferation of prostate cancer cells by activating TRPM7 channels. J Biol Chem 288(1):255–263

Tomisato W, Tanaka K, Katsu T, Kakuta H, Sasaki K, Tsutsumi S, Hoshino T, Aburaya M, Li D, Tsuchiya T, Suzuki K, Yokomizo K, Mizushima T (2004) Membrane permeabilization by non-steroidal anti-inflammatory drugs. Biochem Biophys Res Commun 323(3):1032–1039

Totzke G, Schulze-Osthoff K, Jänicke RU (2003) Cyclooxygenase-2 (COX-2) inhibitors sensitize tumor cells specifically to death receptor-induced apoptosis independently of COX-2 inhibition. Oncogene 22(39):8021–8030

Wangemann P, Wittner M, Di Stefano A, Englert HC, Lang HJ, Schlattder E, Greger R (1986) Cl(−)-channel blockers in the thick ascending limb of the loop of Henle. Structure activity relationship. Pflugers Arch 407(Suppl 2):S128–S141

Zhang GS, Liu DS, Dai CW, Li RJ (2006) Antitumor effects of celecoxib on K562 leukemia cells are mediated by cell-cycle arrest, caspase-3 activation, and downregulation of Cox-2 expression and are synergistic with hydroxyurea or imatinib. Am J Hematol 81(4):242–255